arXiv:physics/0508235v1 [physics.optics] 31 Aug 2005

Classification of dispersion equations for homogeneous dielectric–magnetic uniaxial materials

Ricardo A. Depine[1(a,b)], **Marina E. Inchaussandague**[2(a,b)] **and Akhlesh Lakhtakia**[3(c)]

(a) GEA — Grupo de Electromagnetismo Aplicado, Departamento de Física,
Facultad de Ciencias Exactas y Naturales, Universidad de Buenos Aires,
Ciudad Universitaria, Pabellón I, 1428 Buenos Aires, Argentina
(b) CONICET — Consejo Nacional de Investigaciones Científicas y Técnicas,
Rivadavia 1917, Buenos Aires, Argentina
(c) CATMAS — Computational and Theoretical Materials Sciences Group,
Department of Engineering Science and Mechanics,
Pennsylvania State University, University Park, PA 16802–6812, USA

ABSTRACT

The geometric representation at a fixed frequency of the wavevector (or dispersion) surface $\omega(\vec{k})$ for lossless, homogeneous dielectric–magnetic uniaxial materials is explored, when the elements of the relative permittivity and permeability tensors of the material can have any sign. Electromagnetic plane waves propagating inside the material can exhibit dispersion surfaces in the form of ellipsoids of revolution, hyperboloids of one sheet, or hyperboloids of two sheets. Furthermore, depending on the relative orientation of the optic axis, the intersections of these surfaces with fixed planes of propagation can be circles, ellipses, hyperbolas, or straight lines. The obtained understanding is used to study the reflection and refraction of electromagnetic plane waves due to a planar interface with an isotropic medium.

Key words: Anisotropy, Negative refraction, Elliptic dispersion equation, Hyperbolic dispersion equation, Uniaxial material, Indefinite constitutive tensor

1 Introduction

Recent developments in mesoscopic (i.e., structured but effectively homogeneous) materials have significantly broadened the range of available electromagnetic constitutive properties, thereby allowing the realization of solutions to Maxwell's equations which could have been previously regarded

[1]E-mail: rdep@df.uba.ar
[2]Corresponding Author. E-mail: mei@df.uba.ar
[3]E-mail: akhlesh@psu.edu

as mere academic exercises. Materials having effectively negative real permittivity and permeability have been constructed [1, 2, 3] from arrays of conducting wires [4] and arrays of split ring resonators [5]. Such composite materials — often called metamaterials — exhibit a negative index of refraction in certain frequency regimes [6]. Under these conditions, the phase velocity vector is in the opposite direction of the energy flux, for which reason they have been called *negative–phase–velocity* (NPV) materials [7, 8].

NPV metamaterials synthesized thus far are actually anisotropic in nature, and any hypothesis about their isotropic behavior holds only under some restrictions on propagation direction and polarization state. In anisotropic NPV materials, the directions of power flow and phase velocity are not necessarily antiparallel but — more generally — have a negative projection of one on the other [9]. Since the use of anisotropic NPV materials offers flexibility in design and ease of fabrication, attention has begun to be drawn to such materials [10, 11, 12, 13].

Natural crystals are characterized by permittivity and permeability tensors with the real part of all their elements positive, a fact that leads to dispersion equations in the form of closed surfaces. On the other hand, a relevant characteristic of NPV metamaterials is that the real parts of the elements of their permittivity and permeability tensors can have different signs in different frequency ranges. As an example, Parazzoli *et al.* [2] demonstrated negative refraction using s–polarized microwaves and samples for which the permittivity and permeability tensors have certain eigenvalues that are negative real. Under such circumstances, dispersion equations are topologically similar to *open* surfaces [14]. Consequently, the intersection of a dispersion surface and a fixed plane of propagation may be a curve of an unusual shape, compared with its analogs for natural crystals. For example, extraordinary plane waves in a simple dielectric (nonmagnetic) uniaxial medium can exhibit dispersion curves which are hyperbolic, instead of the usual elliptic curves characteristic of natural uniaxial crystals [14, 15]. In recent studies on the characteristics of anisotropic materials with hyperbolic dispersion curves, new phenomenons have been identified, such as omnidirectional reflection — either from a single boundary [10] or from multilayers [16] — and the possibility of an infinite number of refraction channels due to a periodically corrugated surface [17, 18].

In this paper, we are interested in studying the conditions under which the combination of permittivity and permeability tensors with the real parts of their elements of arbitrary sign, leads to closed or open dispersion surfaces for a homogeneous dielectric–magnetic uniaxial material. To

characterize this kind of material, four constitutive scalars are needed:

- $\epsilon_\parallel$ and $\mu_\parallel$, which are the respective elements of the relative permittivity and relative permeability tensors along the optic axis; and
- $\epsilon_\perp$ and $\mu_\perp$, which are the elements of the two tensors in the plane perpendicular to the optic axis.

These scalars have positive real parts for natural crystals, but their real parts can have any sign for artificial (but still effectively homogeneous) materials. The dispersion equation for plane waves in such a material can be factorized into two terms, leading to the conclusion that the material supports the propagation of two different types of linearly polarized waves, called magnetic and electric modes [19, 20].

The relative permittivity and permeability tensors, $\tilde{\epsilon}$ and $\tilde{\mu}$, are real symmetric when dissipation can be ignored. Then, each tensor can be classified as [21]:

(i) positive definite, if all eigenvalues are positive;

(ii) negative definite, if all eigenvalues are negative; and

(iii) indefinite, if it has both negative and positive eigenvalues.

Thus, the relative permittivity tensor is positive definite if $\epsilon_\perp > 0$ and $\epsilon_\parallel > 0$; it is negative definite if $\epsilon_\perp < 0$ and $\epsilon_\parallel < 0$; and it is indefinite if $\epsilon_\perp \epsilon_\parallel < 0$. In the present context, we exclude constitutive tensors with null eigenvalues. A similar classification applies to the relative permeability tensor. If both $\tilde{\epsilon}$ and $\tilde{\mu}$ are positive definite, the material is of the positive–phase–velocity (PPV) kind.

The plan of this paper is as follows. Considering the different possible combinations of $\tilde{\epsilon}$ and $\tilde{\mu}$, we show in Section 2 that magnetic and electric propagating modes can exhibit dispersion surfaces which are

(a) ellipsoids of revolution,

(b) hyperboloids of one sheet, or

(c) hyperboloids of two sheets.

As a byproduct of our analysis, we also obtain different possible combinations of $\tilde{\epsilon}$ and $\tilde{\mu}$ that preclude the propagation of a mode — either electric, magnetic or both — inside the material. In Section 3 we study the intersection between the dispersion surfaces and a fixed plane of propagation that is arbitrarily oriented with respect to the optic axis. We show that, depending on the relative orientation of the optic axis, different dispersion curves, in the form of circles, ellipses, hyperbolas or even straight lines, can be obtained. Previous studies on dielectric–magnetic materials with indefinite constitutive tensors only considered planes of propagation coinciding with coordinate planes, thus failing to identify the singular case of linear dispersion equations. These results are used in Section 4 to discuss the reflection and refraction of electromagnetic plane waves due to a planar interface between a dielectric–magnetic uniaxial material and an isotropic medium. Concluding remarks are provided in Section 5. An $\exp(-i\omega t)$ time–dependence is implicit, with ω as angular frequency, t as time, and $i = \sqrt{-1}$.

2 Dispersion surfaces

The relative permeability and permittivity tensors of the anisotropic medium share the same optic axis denoted by the unit vector $\hat{c}$, and their four eigenvalues are denoted by $\epsilon_{\perp,\parallel}$ and $\mu_{\perp,\parallel}$. In dyadic notation [23]

$$\left.\begin{array}{l} \tilde{\epsilon} = \epsilon_\perp \tilde{I} + (\epsilon_\parallel - \epsilon_\perp)\, \hat{c}\, \hat{c} \\ \tilde{\mu} = \mu_\perp \tilde{I} + (\mu_\parallel - \mu_\perp)\, \hat{c}\, \hat{c} \end{array}\right\}, \tag{1}$$

with $\tilde{I}$ the identity dyadic. In this medium, two distinct plane waves can propagate in any given direction:

(i) electric modes, with dispersion equation

$$\vec{k} \cdot \tilde{\epsilon} \cdot \vec{k} = k_0^2\, \mu_\perp \epsilon_\perp \epsilon_\parallel \,, \tag{2}$$

and

(ii) magnetic modes, with dispersion equation

$$\vec{k} \cdot \tilde{\mu} \cdot \vec{k} = k_0^2\, \mu_\perp \epsilon_\perp \mu_\parallel \,. \tag{3}$$

Here $\vec{k}$ is the wavevector and k_0 denotes the free–space wavenumber.

We decompose the wavevector $\vec{k} = \vec{k}_\parallel + \vec{k}_\perp$ into its components parallel ($\vec{k}_\parallel$) and perpendicular ($\vec{k}_\perp$) to the optic axis. After taking into account that

$$\vec{k} \cdot \tilde{\epsilon} \cdot \vec{k} = \epsilon_\perp \, (\vec{k} \times \hat{c})^2 + \epsilon_\parallel \, (\vec{k} \cdot \hat{c})^2, \tag{4}$$

(2) for electric modes can be rewritten as

$$\frac{k_\perp^2}{\epsilon_\parallel} + \frac{k_\parallel^2}{\epsilon_\perp} = k_0^2 \, \mu_\perp \, . \tag{5}$$

Analogously, (3) for magnetic modes can be expressed as

$$\frac{k_\perp^2}{\mu_\parallel} + \frac{k_\parallel^2}{\mu_\perp} = k_0^2 \, \epsilon_\perp \, . \tag{6}$$

Equations (5) and (6) have both the quadric form

$$\frac{k_\perp^2}{A} + \frac{k_\parallel^2}{B} = 1 \, , \tag{7}$$

which displays symmetry of revolution about the $k_\parallel$ axis in three–dimensional $\vec{k}$–space. The parameters A and B depend on the kind of mode (electric or magnetic) and their values determine the propagating or evanescent character of each mode and the geometric nature of the dispersion surface for propagating modes.

One of the following conditions applies for a specific mode:

(i) $A > 0$ and $B > 0$: the dispersion surface is an ellipsoid of revolution;

(ii) $A > 0$ and $B < 0$: the dispersion surface is an hyperboloid of one sheet (Figure 1a);

(iii) $A < 0$ and $B > 0$: the dispersion surface is an hyperboloid of two sheets (Figure 1b);

(iv) $A < 0$ and $B < 0$: the mode is evanescent.

Depending on the particular combination of $\tilde{\epsilon}$ and $\tilde{\mu}$, we obtain from these conditions different dispersion surfaces. For example, the dispersion equations for electric and magnetic modes in natural crystals are both represented by eq. 7 with $A > 0$ and $B > 0$, a fact that leads to the known result that electric and magnetic modes have dispersion surfaces in the form of either prolate or oblate ellipsoids of revolution. The same result is obtained for metamaterials with both constitutive tensors negative definite. When the analysis is repeated for all possible combinations between the four constitutive scalars $\epsilon_\perp$, $\epsilon_\parallel$, $\mu_\perp$ and $\mu_\parallel$, the results summarized in Table 1 are obtained.

3 Intersection with a fixed plane of propagation

In the previous section, by considering plane wave propagation in an unbounded medium, we found the various geometric forms of the dispersion surfaces. At a specularly flat interface between two half-spaces filled with linear homogeneous materials, the tangential components of the wavevectors of the incident, transmitted and reflected plane waves must all be equal, and consequently, they all must lie in the same plane that is orthogonal to the interface. This plane is the *plane of propagation*. Let us now investigate the kinds of dispersion curves obtained when dispersion surfaces of the kind identified in Section 2 intersect by a specific plane of propagation, arbitrarily oriented with respect to the optic axis $\hat{c}$.

Without loss of generality, let the xy plane be the fixed plane of propagation in a cartesian coordinate system; furthermore, let $\hat{c} = c_x\hat{x} + c_y\hat{y} + c_z\hat{z}$ and $\vec{k} = k_x\hat{x} + k_y\hat{y}$. The dispersion equation (2), for electric modes, can then be rewritten as the quadratic equation

$$M_{11}\, k_x^2 + 2\, M_{12}\, k_x\, k_y + M_{22}\, k_y^2 = F \;, \tag{8}$$

where

$$\left.\begin{array}{l} M_{11} = \epsilon_\perp + (\epsilon_\parallel - \epsilon_\perp) c_x^2 \\ M_{12} = (\epsilon_\parallel - \epsilon_\perp) c_x\, c_y \\ M_{22} = \epsilon_\perp + (\epsilon_\parallel - \epsilon_\perp) c_y^2 \\ F = k_0^2\, \epsilon_\parallel \epsilon_\perp\, \mu_\perp \end{array}\right\} . \tag{9}$$

The dispersion equation (3) for magnetic modes also has the same quadratic form, but now the coefficients M_{11}, M_{12}, M_{22}, and F are obtained by the interchange $\left\{\epsilon_\parallel \longleftrightarrow \mu_\parallel, \epsilon_\perp \longleftrightarrow \mu_\perp\right\}$ in (9).

The symmetric matrix

$$\tilde{M} = \left[\begin{array}{cc} M_{11} & M_{12} \\ M_{12} & M_{22} \end{array}\right] , \tag{10}$$

corresponding to the quadratic equation (8) is defined by its three elements. This matrix can be diagonalized by rotating the xy plane about the z axis by a certain angle, thereby eliminating the $k_x k_y$ term in (8). With $\hat{v}_1$ and $\hat{v}_2$ denoting the orthonormalized eigenvectors of the matrix $\tilde{M}$, we can write $\vec{k} = k_1\hat{v}_1 + k_2\hat{v}_2$. Likewise, with

$$\left.\begin{array}{l} \lambda_1 = \epsilon_\perp + (\epsilon_\parallel - \epsilon_\perp)(c_x^2 + c_y^2) \\ \lambda_2 = \epsilon_\perp \end{array}\right\} . \tag{11}$$

denoting the eigenvalues of $\tilde{M}$, we get the dispersion curve

$$\lambda_1\, k_1^2 + \lambda_2\, k_2^2 = F \tag{12}$$

in the plane of propagation.

The dispersion curves for the mode represented by (12) can be classified by analyzing the signs of λ_1, λ_2 and F. In particular,

(i) if λ_1, λ_2 and F all have the same sign, then the dispersion curve in the fixed plane of propagation is an ellipse, with semiaxes along the directions $\hat{v}_1$ and $\hat{v}_2$;

(ii) if λ_1 and λ_2 have both the same sign, but F has the opposite sign, then the mode represented by (12) is of the evanescent kind;

(iii) if λ_1 and λ_2 have opposite signs, then the dispersion curve is a hyperbola, with semiaxes along the directions $\hat{v}_1$ and $\hat{v}_2$;

(iv) if one eigenvalue is equal to zero and the other (nonzero) eigenvalue has the same sign as F, then the dispersion curve is a straight line, parallel to the eigenvector associated with the null eigenvalue.

4 Illustrative numerical results and discussion

To illustrate the different possibilities for the dispersion curves, let us present numerical results for the following two cases:

Case I: $\epsilon_\perp = -2.1$, $\epsilon_\parallel = 1.9$, $\mu_\perp = 1.3$ and $\mu_\parallel = -1.6$;

Case II: $\epsilon_\perp = 2.1$, $\epsilon_\parallel = -1.9$, $\mu_\perp = -1.3$ and $\mu_\parallel = 1.6$.

Both constitutive tensors thus are chosen to be indefinite. According to Table 1, the electric and magnetic modes for both Case I and Case II have dispersion surfaces in the form of one–sheet hyperboloids of revolution, whose intersections with fixed planes of propagation are circles, ellipses, hyperbolas or straight lines — depending on the orientation of $\hat{c}$.

Furthermore, to show the usefulness of our analysis in visualizing dispersion curves for boundary value problems, let us now consider that the anisotropic medium is illuminated by a plane wave from a vacuous half–space, the plane of incidence being the xy plane. In terms of (a) the angle θ_c

between the optic axis and the y axis and (b) the angle φ_c between the x axis and the projection of the optic axis onto the xy plane, the optic axis can be stated as

$$\hat{c} = \hat{x}\sin\theta_c\,\cos\varphi_c + \hat{y}\cos\theta_c + \hat{z}\sin\theta_c\,\sin\varphi_c\ , \tag{13}$$

and the eigenvalues λ_j^E, corresponding to electric modes can be written as

$$\left.\begin{array}{l} \lambda_1^E = \epsilon_\perp + (\epsilon_\parallel - \epsilon_\perp)(1 - \sin^2\theta_c\,\sin^2\varphi_c) \\ \lambda_2^E = \epsilon_\perp \end{array}\right\}\ . \tag{14}$$

For Case I, $F^E < 0$, $\lambda_2^E = \epsilon_\perp < 0$, whereas the sign of λ_1^E depends on the optic axis orientation. From (14) we conclude for the electric modes as follows:

- $\lambda_1^E > 0$ if
$$\sin^2\theta_c\,\sin^2\varphi_c < \frac{\epsilon_\parallel}{\epsilon_\parallel - \epsilon_\perp}\ , \tag{15}$$
and the dispersion curves are hyperbolas with semiaxes along the directions $\hat{v}_1^E$ and $\hat{v}_2^E$;

- $\lambda_1^E = 0$ if
$$\sin^2\theta_c\,\sin^2\varphi_c = \frac{\epsilon_\parallel}{\epsilon_\parallel - \epsilon_\perp}\ , \tag{16}$$
and the dispersion curves are straight lines parallel to the direction associated with the eigenvector $\hat{v}_1^E$; and

- $\lambda_1^E < 0$ if
$$\sin^2\theta_c\,\sin^2\varphi_c > \frac{\epsilon_\parallel}{\epsilon_\parallel - \epsilon_\perp}\ , \tag{17}$$
and the dispersion curves are ellipses with semiaxes along the directions of the eigenvectors $\hat{v}_1^E$ and $\hat{v}_2^E$.

The same conclusions hold for electric modes in Case II.

Analogously, the eigenvalues λ_j^M, corresponding to magnetic modes are as follows:

$$\left.\begin{array}{l} \lambda_1^M = \mu_\perp + (\mu_\parallel - \mu_\perp)(1 - \sin^2\theta_c\,\sin^2\varphi_c) \\ \lambda_2^M = \mu_\perp \end{array}\right\}\ , \tag{18}$$

For Case I, $F^M > 0$ and $\lambda_2^M = \mu_\perp > 0$. From (18) we deduce that

- $\lambda_1^M < 0$ if
$$\sin^2\theta_c\,\sin^2\varphi_c < \frac{\mu_\parallel}{\mu_\parallel - \mu_\perp}\ , \tag{19}$$
and the dispersion curves are hyperbolas with semiaxes along the directions $\hat{v}_1^M$ and $\hat{v}_2^M$;

- $\lambda_1^M = 0$ if

$$\sin^2\theta_c \sin^2\varphi_c = \frac{\mu_\parallel}{\mu_\parallel - \mu_\perp} \ , \tag{20}$$

and the dispersion curves are straight lines parallel to the direction associated of the eigenvector $\hat{v}_1^M$;

- $\lambda_1^M > 0$ if

$$\sin^2\theta_c \sin^2\varphi_c > \frac{\mu_\parallel}{\mu_\parallel - \mu_\perp} \ , \tag{21}$$

and the dispersion curves are ellipses with semiaxes along the directions of the eigenvectors $\hat{v}_1^M$ and $\hat{v}_2^M$.

The same conclusions hold for magnetic modes in Case II.

Let $\varphi_c > 0^\circ$ so that the optic axis is not wholly contained in the plane of incidence. There exist critical values of θ_c at which the dispersion curve change from hyperbolic/elliptic to elliptic/hyperbolic. By virtue of (16), the critical value for electric modes is given by

$$\sin\theta_c^E = \left[\frac{\epsilon_\parallel}{(\epsilon_\parallel - \epsilon_\perp)\sin^2\varphi_c}\right]^{1/2} . \tag{22}$$

Likewise, the critical value

$$\sin\theta_c^M = \left[\frac{\mu_\parallel}{(\mu_\parallel - \mu_\perp)\sin^2\varphi_c}\right]^{1/2} \tag{23}$$

for magnetic modes emerges from (20). Expressions (22) and (23) are valid for both Cases I and II. At a critical value of θ_c, the dispersion curve for the corresponding mode is a straight line.

Suppose $\varphi_c = 60^\circ$, so that $\theta_c^E = 52.73^\circ$ and $\theta_c^M = 59.06^\circ$. Then, for $\theta_c = \theta_c^E$ the dispersion curves in the plane of incidence are straight lines (electric modes) and hyperbolas (magnetic modes); whereas for $\theta_c = \theta_c^M$, the dispersion curves are ellipses (electric modes) and straight lines (magnetic modes).

In Figure 2, the reciprocal space maps for four different orientations of the optic axis are shown:

- $\theta_c = 20^\circ$ (both dispersion curves hyperbolic),
- $\theta_c = \theta_c^E = 52.73^\circ$ (electric type linear and magnetic type hyperbolic),
- $\theta_c = 55^\circ$ (electric type elliptic and magnetic type hyperbolic), and

- $\theta_c = \theta_c^M = 59.06^\circ$ (electric type elliptic and magnetic type linear).

For $\theta_c > \theta_c^M = 59.06^\circ$, modes of both electric and magnetic types have elliptic dispersion curves — just as for a natural crystal (not shown). The light gray circle in Figure 2 represents the dispersion equation for plane waves in vacuum (the medium of incidence).

For $\theta_c = 20^\circ$, Figure 2a indicates the nonexistence of real–valued k_y in the refracting anisotropic medium for either the electric or the magnetic modes, the specific k_x being indicated by a dashed vertical line in the figure. This is true for both Cases I and II, for any angle of incidence (with respect to the y axis), and for any incident polarization state; hence, the chosen anisotropic medium behaves as an omnidirectional total reflector [10]. As the present–day construction of NPV metamaterials is such that the boundary is periodically stepped [24], it is worth noting that the introduction of a periodic modulation along the surface would subvert the omnidirectional reflector effect, since a periodic modulation allows for the presence of spatial harmonics with tangential components of their wavevectors that can now satisfy the required matching condition. Gratings of this kind, contrary to what happens for all gratings made of conventional materials, have been recently shown to support an infinite number of refracted channels [17, 18].

When $\theta_c = \theta_c^E = 52.73^\circ$ the dispersion equation for refracted modes of the electric type is linear. It is posible to find two wavevectors with real–valued components that satisfy the phase–matching condition (the so–called Snell's law) at the interface, one belonging to the upper straight line and the other to the lower straight line in Figure 2b. As the direction of the time–averaged Poynting vector associated with electric modes is given by [20]

$$\vec{S} = \frac{\omega\,\epsilon_\perp}{8\pi\,\epsilon_\parallel}(\vec{k}\times\hat{c})^2\,\tilde{\epsilon}\cdot\vec{k}\,, \tag{24}$$

we conclude that the refracted wavevectors on the upper straight line do not satisfy the radiation condition for Case I, whereas wavevectors on the lower straight line do not satisfy the radiation condition for Case II.

The direction of $\vec{S}$ given by (24) for modes of the electric type is normal to the dispersion curves and points towards $y < 0$, as required by the radiation condition. Ray directions coincide with the direction of $\vec{S}$. As for the parameters considered in our examples, the z component of the time–averaged Poynting vector does not vanish, the ray directions are not contained in the plane of incidence. The projections of the refracted rays onto the xy plane (indicated by little arrows in

the figures) are perpendicular to the straight lines and independent of the angle of incidence.

For refracted modes of the magnetic type and for the angle of incidence ($= \sin^{-1} k_x/k_o$) shown in Figure 2b, it is also posible to find two refracted wavevectors with real–valued components satisfying the phase–matching condition at the interface, one belonging to the upper hyperbola (not shown) and the other to the lower hyperbola. The time–averaged Poynting vector associated with the magnetic modes is given by

$$\vec{S} = \frac{\omega}{8\pi k_0^2} \frac{(\vec{k} \times \hat{c})^2}{\mu_\perp \mu_\parallel} \, \tilde{\mu} \cdot \vec{k} \, . \tag{25}$$

Therefore, we conclude that wavevectors on the upper hyperbola do not satisfy the radiation condition for Case II, whereas wavevectors on the lower hyperbola do not satisfy the radiation condition for Case I. Ray directions coincide with the direction of $\vec{S}$ given by 25, which again has a non–zero component in the z direction. Ray projections onto the xy plane (indicated by little arrows in the figures) are perpendicular to the hyperbolas.

The interface for both Cases I and II acts as a positively refracting interface for modes of both types, in the sense that the refracted rays never emerge on the same side of the normal as the incident ray [22].

When the angle θ_c is increased to 55° (Figure 2c), the dispersion equation for the refracted modes of the magnetic type is still hyperbolic, but the dispersion equation for the electric type is elliptic. Again, for both electric and magnetic modes, is it possible to find two wavevectors with acceptable real–valued components. From (24), we conclude that refracted electric modes on the upper part of the ellipse correspond to Case II, whereas electric wavevectors on the lower part of the ellipse correspond to Case I. On the other hand, wavevectors for the refracted magnetic modes on the upper hyperbola do not satisfy the radiation condition for Case II, whereas wavevectors on the lower hyperbola do not satisfy the radiation condition for Case I, as can be deduced from (25).

Ray projections onto the xy plane corresponding to the magnetic modes alone are shown in the figure, for the sake of clarity. For both Cases I and II and for refracted modes of the electric and magnetic types, the refracted rays never emerge on the same side of the y axis as the incident ray, just as for positively refracting interfaces.

When $\theta_c = \theta_c^M = 59.06°$ (Figure 2d), the dispersion curves for the refracted modes of the electric type continue to be ellipses, but now the dispersion curves for the modes of the magnetic

type become straight lines. For the electric modes, the selection of the wavevectors is identical to that in Figure 2c. For the refracted magnetic modes, wavevectors on the upper straight line do not satisfy the radiation condition for Case II, whereas wavevectors on the lower straight line do not satisfy the radiation condition for Case I.

Ray projections onto the xy plane for the refracted magnetic modes are also drawn in the figure. Again, for both Cases I and II the surface acts as a positively refracting interface for modes of both types.

5 Concluding remarks

This work focused on the geometric representation at a fixed frequency of the dispersion surface $\omega(\vec{k})$ for lossless, homogeneous dielectric–magnetic uniaxial materials. To encompass both natural crystals and the artificial composites used to demonstrate negative refraction (metamaterials), we assumed that the elements of the permittivity and permeability tensors characterizing the material can have any sign. We showed that, depending on a particular combination of the elements of these tensors, the propagating electromagnetic modes supported by the material can exhibit dispersion surfaces in the form of (a) ellipsoids of revolution, (b) hyperboloids of one sheet, or (c) hyperboloids of two sheets. Intersections of these surfaces with fixed planes of propagation lead to circles, ellipses, hyperbolas or straight lines, depending on the relative orientation of the optic axis. This analysis was used to discuss the reflection and refraction of electromagnetic plane waves due to a planar interface with vacuum (or any linear, homogeneous, isotropic, dielectric–magnetic medium).

Acknowledgments RAD and MEI acknowledge financial support from Consejo Nacional de Investigaciones Científicas y Técnicas (CONICET), Agencia Nacional de Promoción Científica y Tecnológica (ANPCYT-BID 1201/OC-AR-PICT14099) and Universidad de Buenos Aires. AL is grateful for financial support from the Penn State CIRTL project.

References

[1] R. A. Shelby, D. R. Smith, and S. Schultz, "Experimental verification of negative index of refraction," Science **292**, 77–79 (2001).

[2] C. G. Parazzoli, R. B. Greegor, K. Li, B. E. C. Koltenbah, and M. Tanielian, "Experimental verification and simulation of negative index of refraction using Snell's law," Phys. Rev. Lett. **90**, 1074011–1074014 (2003).

[3] A. A. Houck , J. B. Brock, and I. L. Chuang, "Experimental observations of a left–handed material that obeys Snell's law," Phys. Rev. Lett. **90**, 1374011–1374014 (2003).

[4] J. B. Pendry, A. J. Holden, W. J. Stewart, and I. Youngs, "Extremely low frequency plasmons in metallic mesostructures," Phys. Rev. Lett. **76**, 4773–4776 (1996).

[5] J. B. Pendry, A. J. Holden, and W. J. Stewart, "Magnetism from conductors and enhanced nonlinear phenomena," IEEE Trans. Microw. Theory Tech. **47**, 2075–2084 (1999).

[6] A. Lakhtakia, M. W. McCall and W. S. Weiglhofer, "Brief overview of recent developments on negative phase–velocity mediums (alias left–handed materials)," AEÜ Int. J. Electron. Commun. **56**, 407–410 (2002).

[7] A. Lakhtakia, M. W. McCall and W. S. Weiglhofer, "Negative phase–velocity mediums," in: W. S. Weiglhofer and A. Lakhtakia (eds.), *Introduction to Complex Mediums for Optics and Electromagnetics* (SPIE Press, Bellingham, Wash., 2003).

[8] A. D. Boardman, N. King and L. Velasco, "Negative refraction in perspective," Electromagnetics **25**, 365–389 (2005).

[9] T. G. Mackay and A. Lakhtakia, "Plane waves with negative phase velocity in Faraday chiral mediums," Phys. Rev. E **69**, 0266021–0266029 (2004).

[10] L. B. Hu and S. T. Chui, "Characteristics of electromagnetic wave propagation in uniaxially anisotropic left–handed materials," Phys. Rev. B **66**, 0851081–0851087 (2002).

[11] A. Lakhtakia and J. A. Sherwin, "Orthorhombic materials and perfect lenses," Int. J. Infrared Millim. Waves **24**, 19–23 (2003).

[12] D. R. Smith and D. Schurig, "Electromagnetic wave propagation in media with indefinite permittivity and permeability tensors," Phys. Rev. Lett. **90**, 0774051–0774054 (2003).

[13] D. R. Smith, P. Kolinko, and D. Schurig, "Negative refraction in indefinite media," J. Opt. Soc. Am. B **21**, 1032–1043 (2004).

[14] O. S. Eritsyan, "On the optical properties of anisotropic media in the presence of negative components of dielectric and (or) magnetic tensors," Crystallography Reports **50**, 465–470 (2005).

[15] T. G. Mackay, A. Lakhtakia and R. A. Depine, "Uniaxial dielectric mediums with hyperbolic dispersion relations," arXiv:physics/0506057

[16] Z. Liu, J. Xu and Z. Lin, "Omnidirectional reflection from a slab of uniaxially anisotropic negative refractive index materials," Opt. Commun. **240**, 19–27 (2004).

[17] R. A. Depine and A. Lakhtakia, "Diffraction by a grating made of an uniaxial dielectric magnetic medium exhibiting negative refraction," New J. Phys. **7**, 158 (2005).

[18] R. A. Depine, M. E. Inchaussandague and A. Lakhtakia, "Application of the differential method to uniaxial gratings with an infinite number of refraction channels: scalar case," Opt. Commun. (to be published).

[19] A. Lakhtakia, V. K. Varadan and V. V. Varadan, "Plane waves and canonical sources in a gyroelectromagnetic uniaxial medium," Int. J. Electron. **71**, 853–861 (1991).

[20] A. Lakhtakia, V. K. Varadan and V. V. Varadan, "Reflection and transmission of plane waves at the planar interface of a general uniaxial medium and free space," J. Modern Opt. **38**, 649–657 (1991)

[21] H. Lütkepohl, *Handbook of Matrices* (Chicester, United Kingdom: Wiley, Chicester, United Kingdom, 1996).

[22] A. Lakhtakia A and M. W. McCall, "Counterposed phase velocity and energy–transport velocity vectors in a dielectric–magnetic uniaxial medium," Optik **115**, 28–30 (2004).

[23] H.C. Chen, *Theory of Electromagnetic Waves: A Coordinate–free Approach* (McGraw–Hill, New York, 1983).

[24] R. A. Depine, A. Lakhtakia and D. R. Smith, "Enhanced diffraction by a rectangular grating made of a negative phase–velocity (or negative index) material," Phys. Lett. A **337**, 155–160 (2005)

Table 1: Types of possible dispersion surfaces for different combinations between the eigenvalues $\epsilon_\perp$, $\epsilon_\parallel$, $\mu_\perp$ and $\mu_\parallel$ of the real symmetric tensors $\tilde{\epsilon}$ and $\tilde{\mu}$. The first symbol indicates the mode: E (electric) or M (magnetic). The second symbol indicates the geometrical form of the dispersion surface: e (ellipsoids of revolution), h_1 (hyperboloid of one sheet), h_2 (hyperboloid of two sheets). The symbol n indicates that the corresponding mode is of the evanescent (i.e., nonpropagating) kind.

	$\epsilon_\perp > 0$ $\epsilon_\parallel > 0$	$\epsilon_\perp > 0$ $\epsilon_\parallel < 0$	$\epsilon_\perp < 0$ $\epsilon_\parallel > 0$	$\epsilon_\perp < 0$ $\epsilon_\parallel < 0$
$\mu_\perp > 0$ $\mu_\parallel > 0$	E e M e	E h_2 M e	E h_1 M n	E n M n
$\mu_\perp > 0$ $\mu_\parallel < 0$	E e M h_2	E h_2 M h_2	E h_1 M h_1	E n M h_1
$\mu_\perp < 0$ $\mu_\parallel > 0$	E n M h_1	E h_1 M h_1	E h_2 M h_2	E e M h_2
$\mu_\perp < 0$ $\mu_\parallel < 0$	E n M n	E h_1 M n	E h_2 M e	E e M e

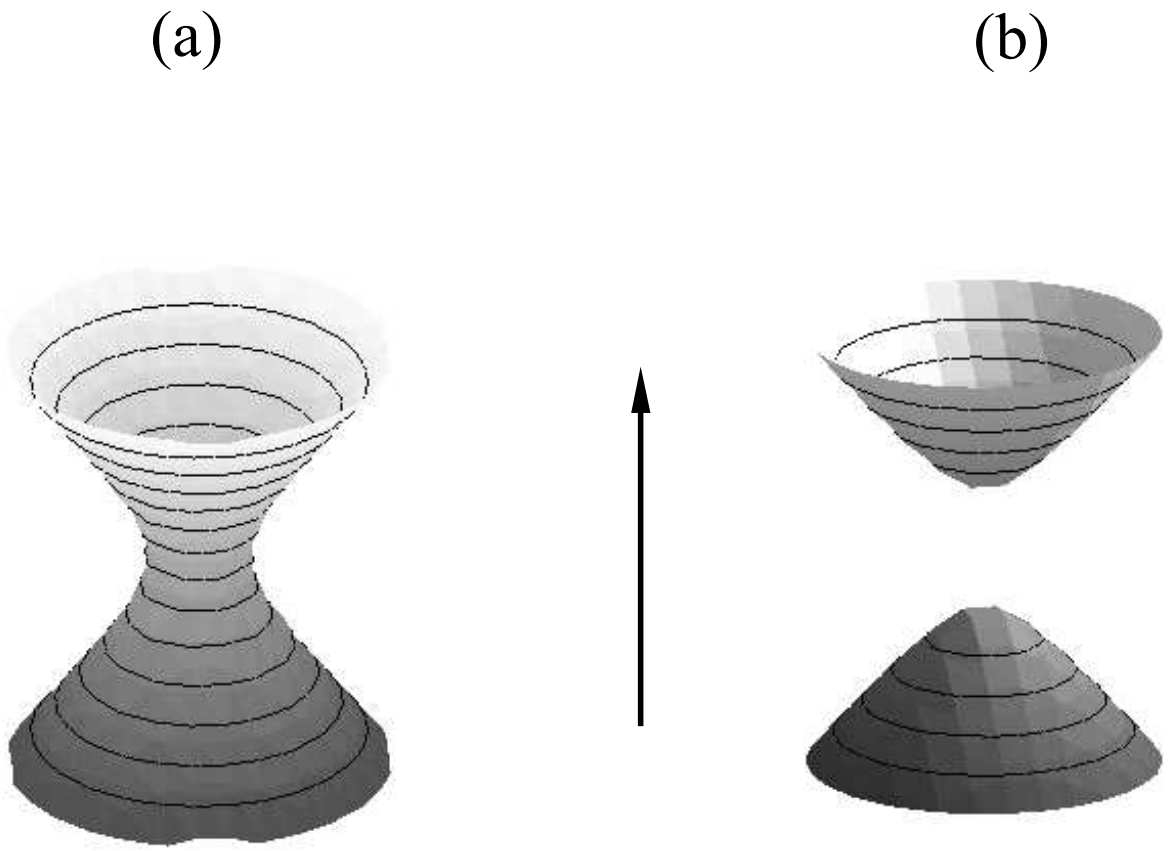

Figure 1: Geometrical representations of (7). (a) $A > 0$ and $B < 0$, hyperboloid of one sheet; (b) $A < 0$ and $B > 0$: hyperboloid of two sheets.

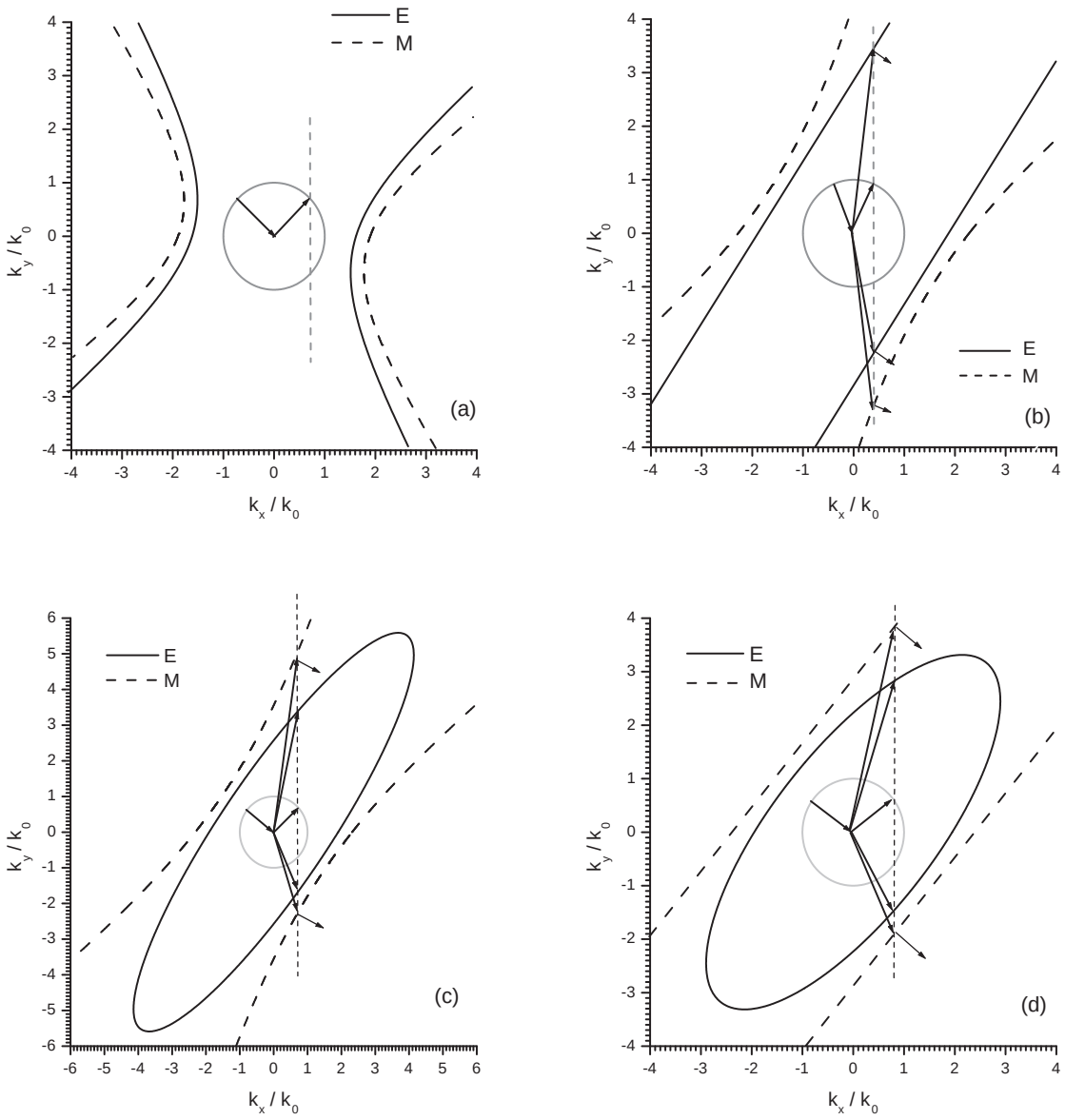

Figure 2: Reciprocal space maps for Cases I and II, when $\varphi_c = 60°$. (a) $\theta_c = 20°$, (b) $\theta_c = 52.73°$, (c) $\theta_c = 55°$, and (d) $\theta_c = 59.06°$. The light gray circle represents the dispersion equation for plane waves in the medium of incidence.